

Accumulated Carrier Density Dependence of Pentacene TFT Mobility Determined by Split C-V Technique

T. Yokoyama, T. Nishimura, K. Kita, K. Kyuno and A. Toriumi

Department of Materials Science, School of Engineering, The University of Tokyo,

7-3-1 Hongo, Tokyo 113-8656, Japan

Phone: +81-3-5841-7161 E-mail: yokoyama@adam.t.u-tokyo.ac.jp

1. Introduction

Pentacene has attracted much attention from its high mobility of organic field-effect transistors [1,2]. However, it is rather questionable about the mobility determination method by the conventional I-V characteristics on the basis of analytical FET model. This paper reports the pentacene mobility determined by the split C-V technique for the first time.

2. Experiments and Results

2.1 Sample Fabrication

The top-contact type capacitors and FETs were fabricated as schematically shown in **Fig. 1**. Each device was fabricated on 31 nm-thick SiO₂ thermally grown on n-silicon substrates. Pentacene film was grown by the vacuum evaporation with deposition rate of 0.05 nm/s and substrate temperature of 25 °C. Au for pentacene and Al for n-Si as electrical contacts were thermally evaporated. The pentacene thickness was 50 nm. Au electrode size was W/L=1000μm/500μm and the channel length was varied from 50 to 300μm. Note that a difference between Fig. 1(a) and (b) is the area of pentacene film. In the case of Fig. 1(a), a rather wide area capacitor is effectively measured as described below.

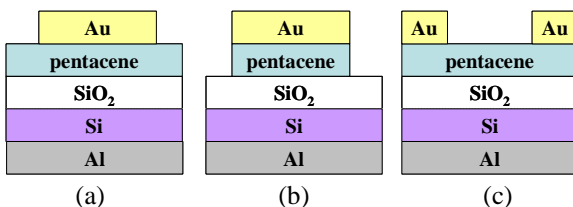


Fig. 1. Schematic diagrams of MIS and FET structures fabricated in this work. The n-silicon was used for gate electrode.

2.2 Frequency Dependent C-V Characteristics of Au/Pentacene/SiO₂/n-Si/Al Capacitors

Fig. 2 shows C-V characteristics measured for type (a) and (b) capacitors in Fig. 1 as a function of measurement frequency. It is noted that there is a big discrepancy between them in spite of having the same Au electrode area. It is explainable by considering that the pentacene film is a highly resistive semiconductor as shown in the inset of Fig. 2 using equivalent circuits. The point is that the effective accumulation area at the SiO₂ interface in Fig. 2(a) as well as the effective dielectric thickness including the pentacene thickness in Fig. 2 (a), (b) have to be considered in terms of a measurement frequency dependence. Thus, in order to evaluate the sheet carrier density at the pentacene/SiO₂ interface by integrating C-V characteristics, it is important to

employ rather low frequency (<1 kHz) and to consider the alignment accuracy of the electrode to the pentacene. It was confirmed that the saturated capacitance in Fig. 2 (b) corresponds to the SiO₂ thickness within 95 % accuracy.

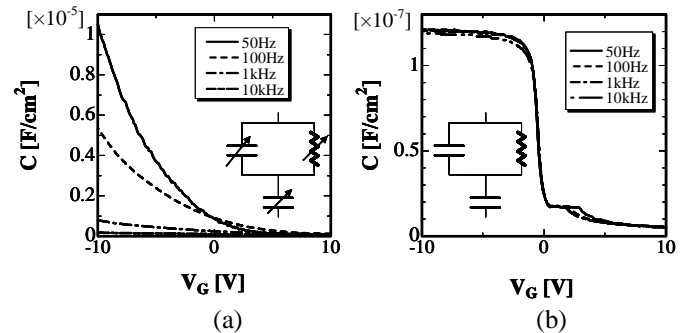


Fig.2 C-V characteristics of capacitor (a) and (b) in Fig.1. C-V characteristics are completely different, though Au electrode areas are exactly the same.

2.3 Channel Capacitance of Pentacene TFT by a Split C-V Technique

A split C-V technique can be used for extract the surface carrier density [3], by integrating gate-to-channel capacitance, C_{GC} which is defined as $C_{GC} = S \cdot dQ_{CH} / dV_{GS}$, where S is the area of accumulation channel and C_{GC} is determined by measuring the ac current with LCR meter in the configuration described in **Fig. 3**.

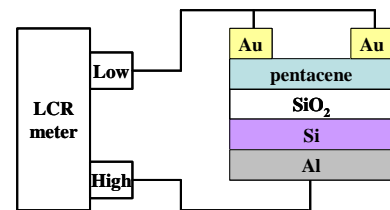


Fig3. Schematic diagram of the split CV measurement system for Au/pentacene/SiO₂/n-Si/Al TFTs. AC signal with amplitude of 100 mV is applied on Al gate with a frequency from 50 Hz to 1 kHz.

In the pentacene TFT in Fig.1 (c), however, the LCR meter measures the ac current component injecting into the channel in addition to the displacement current involved with Au/pentacene/SiO₂/n-Si/Al capacitors at source and drain Au electrodes, because of large overlapped areas between gate (n-Si) and source/drain. To evaluate only the channel capacitance, two channel lengths TFTs with the same size Au electrodes were employed. **Fig. 4** (a) shows a difference of C-V characteristics between capacitors with L=100 μm and L=200 μm. This result has a also measure-

ment frequency dependence, as shown in Fig.4 (a). With this method, only the channel capacitance accumulated at the pentacene/SiO₂ interface can be evaluated by using the frequency independent capacitance component.

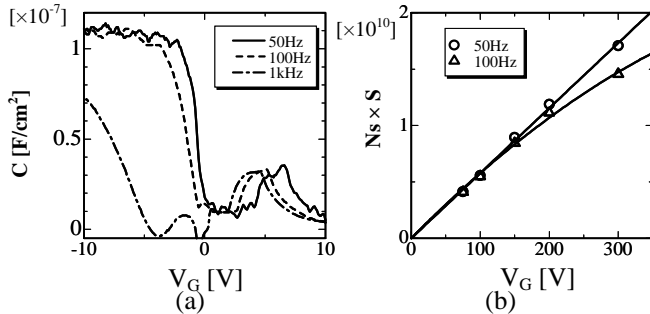


Fig.4. (a) A difference of C-V characteristics between capacitors $L=100 \mu\text{m}$ and $L=200 \mu\text{m}$ for three measurement frequency. (b) The accumulation charge density, N_s , is independent of the measurement frequency below 100 Hz for FETs with channel length shorter than $200 \mu\text{m}$.

The surface carrier density, N_s , was accurately evaluated by integrating C-V characteristics of Fig.4(a). 50 Hz was used for evaluating the channel capacitance, because Fig. 4(b) assures that accumulated charges are in proportion to the channel length at 50 Hz. The DC I-V characteristics were also measured as shown in **Fig. 5**. Since $V_{DS} = -1$ V was applied to evaluate the channel conductance, $N_{CH}(V_{GS}) = [N_s(V_{GS} + N_s(V_{GS} - V_{DS})/2]$ was used for evaluating the average carrier density in the channel. **Fig.6** shows N_{CH} at the interface as a function of V_{GS} . By comparing the results of Fig. 5 with those of Fig. 6, the split C-V mobility is obtained.

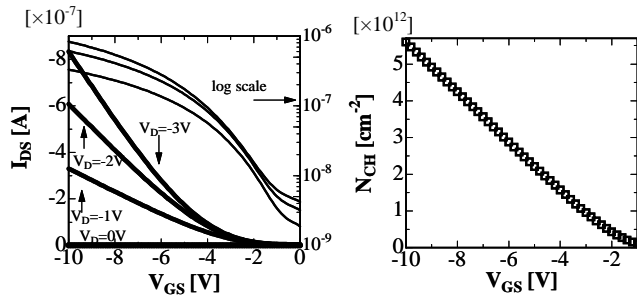


Fig5. I_{DS} - V_{GS} characteristics of $L=100 \mu\text{m}$ TFT shown in Fig.1(c). These characteristics exhibit typical performance of pentacene TFTs.

Fig6. V_{GS} dependence of the average carrier density, N_{CH} . The channel charge density was estimated by integrating CV curve of 50Hz in Fig4.

3. Discussion

The mobility determined by the present method is shown as a function of V_{GS} in **Fig. 7**, together with experimental points of mobility determined by the conventional FET analytical model both in the linear region and in saturation region. The split C-V mobility can provide an overall bias (N_s) dependence of the mobility. The mobilities in the high carrier density region and in the low carrier density region correspond to those in the linear region and in saturation region, respectively. Although the conventional method cannot provide the accumulated carrier density dependence of the mobility in the channel, the present

model can evaluate the overall mobility characteristics as a function of V_{GS} (or N_{CH}). It is clearly shown that the mobility increases with the carrier density in the accumulation layer [2]. In particular, near the threshold voltage the mobility is significantly lowered. This might be due to the effective increase of random potential fluctuations at the boundaries of pentacene grains in the channel at low Q_s region. Generally, the conventional mobility determination by the analytical FET model on the top contact pentacene FET will overestimate the mobility value due to the fact that the finite carrier density near V_{th} is ignored for the carrier density estimation, while the split C-V method accurately counts the carrier number all over the N_s region.

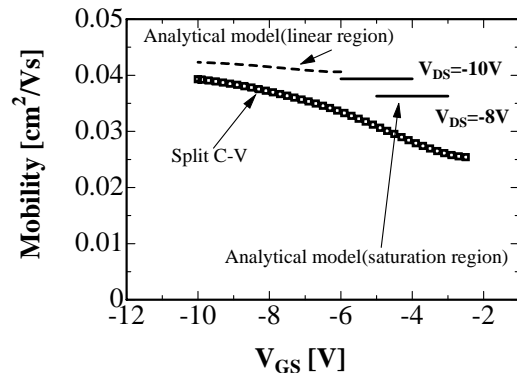


Fig. 7. Three kinds of mobilities as a function of V_{GS} . The Split C-V mobility can provides an overall μ - V_{GS} characteristics.

The method presented in this work will be useful for carrier transport study of organic devices. A concern of this method including the conventional method on the basis of analytical model is the time dependent degradation of FET characteristics. This will be an issue for further study.

4. Conclusion

The pentacene TFT mobility has been accurately determined by the split C-V technique for the first time. The frequency dependence of C-V characteristics should be carefully treated, since pentacene is a highly resistive semiconductor with dielectric properties. With the increase of the carrier density the mobility sharply increases near V_{th} , and gradually increases. The result also verifies that the conventional mobility analysis on the basis of analytical FET model is approximately correct in a limited bias condition. In the low N_s region, the carrier conduction study will be interesting from the viewpoint of the strongly localized carrier transport.

Acknowledgement

This work was partly supported by a Grant-in-Aid for Scientific Research from the Ministry of Education, Culture, Sports, Science and Technology in Japan.

References

- [1] H. Klauk et al., IEEE Trans. Electron Devices **46** (1999) 1258.
- [2] T. Komoda et al., Jpn. J. Appl. Phys. **41** (2002) 2767.
- [3] S. Takagi et al., IEEE Trans. Electron Device, ED-**41** (1994) 2362.